Vibrational modes in electrodeposited amorphous silicon : FT–IR analysis

P. R. L. SARMA, T. R. RAMA MOHAN, S. VENKATACHALAM, V. P. SUNDARSINGH*
*Department of Metallurgical Engineering, and *Department of Electrical Engineering, Indian Institute of Technology, Bombay, 400 076, India*

JAGMAL SINGH
Hardcastle and Waud Mfg Co. Ltd, Netivali Baug, Kalyan, Bombay 421 306, India

Infrared spectra of 13 samples of amorphous silicon bonded with hydrogen, fluorine and carbon, prepared by electrodeposition using a mixture of ethylene glycol and fluosilicic acid were analysed in the wave number region 4000–400 cm^{-1} with a Fourier transform infrared spectrometer. Strong absorption peaks were observed at 1000 cm^{-1} due to the SiF_x stretching mode. Small peaks were seen around 2300 and 640 cm^{-1} due to SiH stretching and wagging modes of absorption. The number of bonded hydrogen atoms in the film deposited at 0.05 M, 50 mA cm^{-2} was calculated to be 6.2579×10^{21} and 1.2302×10^{20} atm cm^{-3} using integrated absorption of the CH and SiH stretching modes, respectively. The absorption coefficient around the SiF_x stretch region was found to vary from 1300–2500 cm^{-1} as the molarity of the electrolyte was increased. Binding energy shifts in X-ray photoelectron spectrum were used as a cross check to confirm the silicon bonding with carbon, hydrogen, oxygen and fluorine atoms. The absence of columnar growth in SEM photographs indicates no polysilane formation in the films.

1. Introduction

It is a widely accepted view that the electrical, optical and structural properties of amorphous silicon (a-Si) films will be significantly affected by the presence of impurities such as hydrogen, carbon and fluorine [1–5]. If so, and whatever be the deposition process, in order to assess the quality of the films, it is essential to have some knowledge of the various impurity atoms and how they are bonded to silicon. Infrared spectroscopy is an important tool for deriving such information. With a wide optical gap (2.8 eV), films of amorphous silicon alloyed with carbon, hydrogen and fluorine (a-Si:C:F:H), have important photovoltaic and luminescent device applications. They may be deposited by glow-discharge decomposition [6] and electrodeposition methods [7, 8].

In the electrodeposition process, it has been reported [7, 8] that the rate of deposition of a-Si is increased at higher molarities and current densities. Before proceeding to analyse the various properties of the electrodeposited films, it is desirable to know the chemical structure of the silicon with respect to impurities at different concentrations and current densities in the electrolyte. With this basic idea, a detailed study has been carried out, possibly for the first time, on the infrared absorption of a-Si:C:F:H thin films obtained by electrodeposition using a Fourier transform infrared spectrometer (FT-IR). The results are corroborated with X-ray photoelectron spectroscopy (XPS) and scanning electron microscopy (SEM) studies.

2. Experimental procedure

Thin films of a-Si containing C, H and F were deposited on stainless steel substrates by electrodeposition using H_2SiF_6 (fluosilicic acid) and ethylene glycol. Samples were obtained under varying conditions of molarity (0.05–0.2 M) and current density (7.5–120 mA cm^{-2}) in the electrolyte. A rectangular mesh of platinum was used as anode. Infrared spectra were obtained using a NICOLET 170 SX FT-IR spectrometer. XPS studies were undertaken using a V G ESCA III Mark II spectrometer with AlK_α X-ray source. A Siemens "Auto Scan" SEM was used for morphological studies.

3. Results and discussion

Table I shows the preparatory conditions of the deposited samples. Figs 1–3 show the transmission spectra of the electrodeposited samples in the wave-number region 4000–400 cm^{-1}. Strong and identical absorptions are seen in these figures at (1) ~ 3400 cm^{-1}, (2) ~ 1600 cm^{-1}, (3) ~ 1000 cm^{-1}, and (4) ~ 800 cm^{-1}. The broad absorption peaks reveal the influence of more than one vibrational mode.

Generally a-Si:F:H alloys can be expected to have various bonding configurations of fluorine to silicon, such as SiF_1, SiF_2, SiF_3, etc. It is, however, difficult to assign the corresponding infrared absorption because the SiF bond stretching vibrations appear in the same frequency region as the SiH bond bending and SiO bond stretching vibrations. In addition, the samples

0022–2461 © 1992 Chapman & Hall

TABLE I Sample preparation conditions

Sample no	Area exposed (cm^2)	Concentration (M)	Current density electrolyte ($mA\ cm^{-2}$)
1	2	0.05	20
2	2	0.05	30
3	2	0.05	40
4	2	0.05	50
5	2	0.10	7.5
6	2	0.10	15
7	2	0.10	25
8	2	0.10	45
9	2	0.10	60
10	2	0.20	25
11	2	0.20	50
12	2	0.20	95
13	2	0.20	120

used in the present study contain carbon in addition to hydrogen, fluorine and oxygen making the systems much more complicated. The present spectra are analysed in the light of the references given in Tables II–IV, the reported reaction mechanism [8], and the additional reactions that are given at the end of the text.

Strong absorption peaks at $1023\ cm^{-1}$ are seen in Figs 1–3. Tindal *et al.* [9] reported the SiF symmetric stretching mode of absorption to be $800–900\ cm^{-1}$, while Venkateswarlu and Sundaram [10] reported it to be at $950–1031\ cm^{-1}$. Similar absorption peaks have been observed at $1015\ cm^{-1}$ by Shimada *et al.* [11] and Fang *et al.* [12] in a-Si:F and a-Si:F:H alloys, respectively. However, there has been much controversy in assigning this absorption to $(SiF_2)_n/SiF_4$ [1, 11–13]. By investigating various experimental and theoretical reports published by Matsumara *et al.* [14], Lucovsky and co-workers [15–17] and others [18–25], on the appearance of frequency doublets in the infrared spectra of a-Si alloys in the region $800–1015\ cm^{-1}$, and also by considering the morphological studies obtained by SEM in these alloys [26–30], it is possible to assign the $1023\ cm^{-1}$ absorption to SiF_4 asymmetric stretch. This assignment is supported by (a) the absence of paired absorption frequencies in the above figures in the $800–1030\ cm^{-1}$ region and (b) the absence of columnar growth in the scanning electron micrographs of the films in the present study. Fig. 4 shows a typical (sample 3) scanning electron micrograph with no columnar growth. The above two points indicate the absence of polysilane $(SiX_2)_n$ structures in the electrodeposited films. A third point which supports the above assignment is found from the XPS studies of the samples with the appearance of an Si-2P peak shift due to SiF_4, as discussed later. Fang *et al.* [12] and Matsumara *et al.* [29] have also assigned the $1015\ cm^{-1}$ absorption to SiF_4 molecules. The apparent shift of this peak in the above figures from $1015\ cm^{-1}$ to $1023\ cm^{-1}$ by a few wave numbers is due to the complexity of the present system which also contains carbon atoms in addition to hydrogen, fluorine and oxygen atoms. Morimoto *et al.* [6] observed the multifluoride stretch at $1035\ cm^{-1}$ in a-Si:C:F:H, which indicates a further shift in frequency of absorption. Further, Mohan and Kroger have observed $1085\ cm^{-1}$ absorption due to $(CH_2)_2SiF_4$ in their electrodeposition studies of a-Si [4], and Jones [31] observed very strong and weak absorptions at 1031 and $1065\ cm^{-1}$, respectively, in the infrared spectra of SiF_4.

In the above figures, the weak absorption at $806\ cm^{-1}$ is due to SiF stretching, and that at

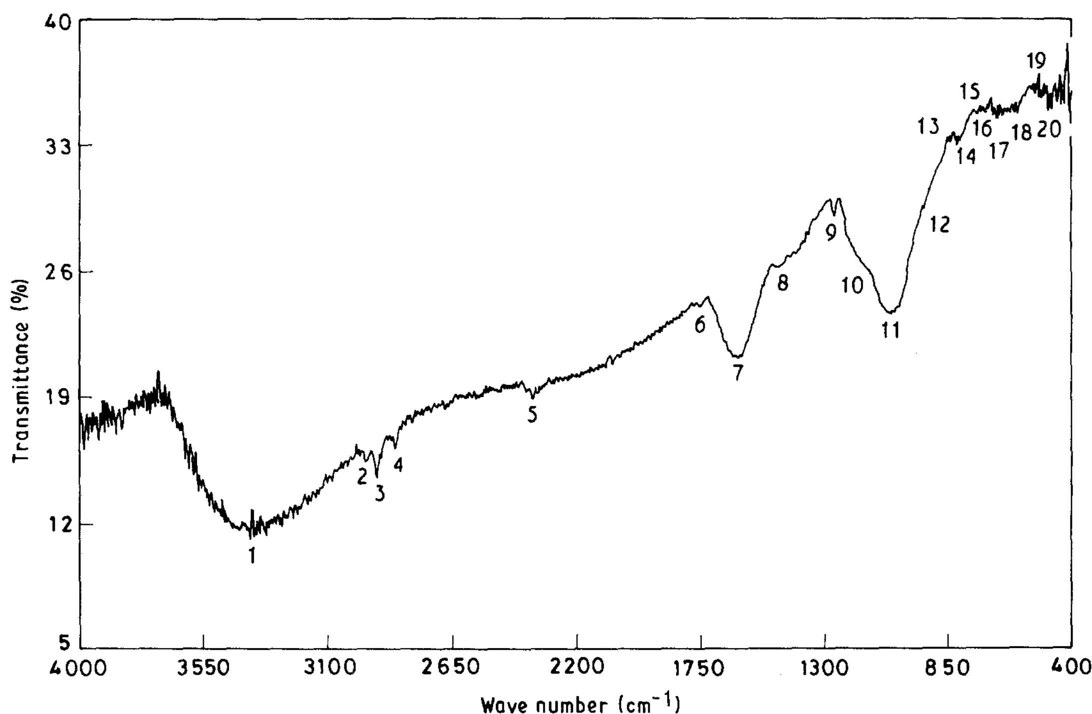

Figure 1 Infrared transmission spectrum of Sample 2. Peak positions (cm^{-1}): (1) 3400, (2) 2962, (3) 2927, (4) 2875, (5) 2340, (6) 1740, (7) 1620, (8) 1455, (9) 1266, (10) 1145, (11) 1023, (12) 920, (13) 840, (14) 823, 806, (15) 730, (16) 711, (17) 677, 660, 635, (18) 580, 546, (19) 504, (20) 485, 465, 450, 430.

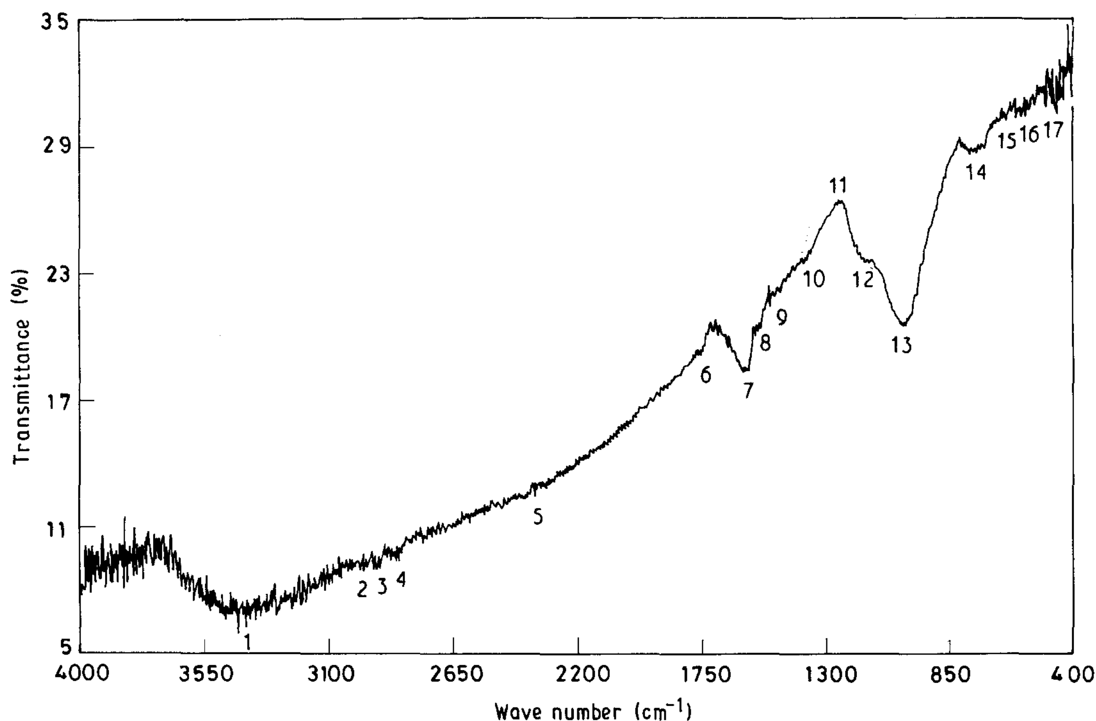

Figure 2 Infrared transmission spectrum of Sample 3. Peak positions (cm^{-1}): (1) 3400, (2) 2962, (3) 2927, (4) 2875, (5) 2338, (6) 1740, (7) 1612, (8) 1560, (9) 1473, (10) 1368, (11) 1260, (12) 1145, (13) 1023, (14) 840, 822, 806, (15) 730, 711, (16) 677, 660, 635, (17) 580, 550, 504, 486, 465, 450, 430.

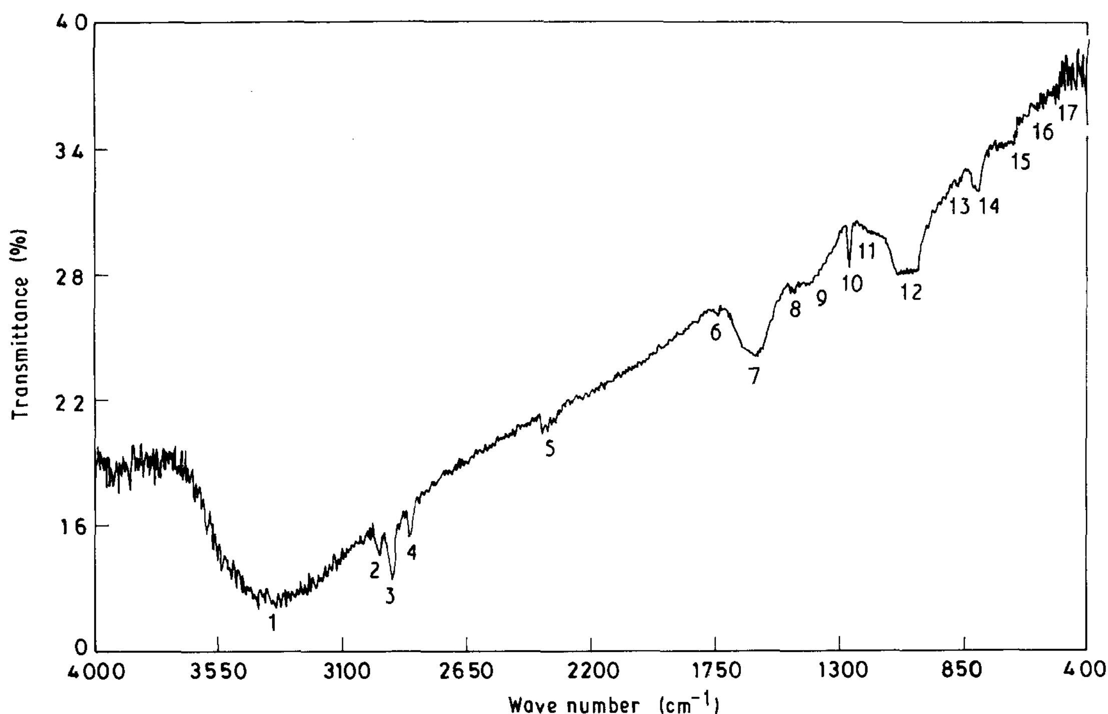

Figure 3 Infrared transmission spectrum of Sample 4. Peak positions (cm^{-1}): (1) 3400, (2) 2962, (3) 2927, (4) 2875, (5) 2345, (6) 1740, (7) 1612, (8) 1456, (9) 1330, (10) 1265, (11) 1145, (12) 1023, (13) 880, 840, (14) 823, 806, (15) 730, 711, 677, 660, (16) 580, 546, 504, (17) 485, 465, 450, 430.

823 cm^{-1} is due to the symmetric stretching of isolated SiF_2 species [11, 12, 14, 15]. The 840 cm^{-1} absorption may be due to SiF_3 for which, according to Shimada *et al.* [11], the symmetric stretching is seen at 838 cm^{-1}. There is a weak absorption band at 880 cm^{-1} in Fig. 3. From the comparisons made by Tindal *et al.* [9] and also by considering the reports given in Table II [2, 5, 12], it may be possible to assign this weak band to an SiF_4 symmetric stretching mode. The presence of SiF_x symmetric stretching modes of absorption in the above spectra gives an indication of the corresponding SiF_x asymmetric stretching modes, also to be included in the broad absorption region (extended up to 950 cm^{-1}) of the peak situated at around 1020 cm^{-1}. From the above figures, it can be seen that the concentration of SiF_x

TABLE II Infrared data in the region ~ 900–1200 cm^{-1}

Sample no.	Wave number (cm^{-1})	Corresponding assignment	Specimen	Reference
1	1015, 995, 830	SiF_x stretching	a-Si:F:H	[2]
2	1010, 920, 830	SiF_4, SiF_2, SiF_1 stretching	a-Si:F:H	[5]
3	1035	Si-multifluoride stretching	a-Si:C:F:H	[6]
4	1015, 930, 820	SiF_4, SiF_3, SiF	a-Si:F:H	[12]
5	1015, 838	SiF_3 asymmetric stretch, SiF_3 symmetric stretching	a-Si:F	[11]
6	965, 920	SiF_2 antisymmetric stretching	a-Si:F	[11]
7	870, 827	SiF_2 symmetric stretching	a-Si:F	[11]
8	1065, 1031	SiF_4 stretching	SiF_4	[31]
9	920	Si–H bending	a-Si:H	[1]
10	900	Si–H bending	a-Si:F:H	[2]
11	930	Si–H bending	a-Si:H	[41]
12	950	Si–H deformation	a-Si (electrodeposited)	[4]
13	900	H–Si–H scissors	a-Si:H:F	[3]

TABLE III Infrared data in the region ~ 400–800 cm^{-1}

Sample no.	Wave number (cm^{-1})	Corresponding assignment	Specimen	Reference
1	700	SiC stretching	a-Si:H:C	[44]
2	700	SiC stretching	a-Si:C	[45]
3	790	$(CH_3)_2SiF_2$	a-Si (electrodeposited)	[4]
4	770	CH_3 rocking	a-Si (electrodeposited)	[4]
5	640	SiH wagging	a-Si:H:F	[2]
6	650	SiH wagging	a-Si:H	[48]
7	630	SiH wagging	a-Si alloy	[18]
8	635	SiH wagging	a-Si:H:F	[12]
9	502	SiTO	a-Si:H:F	[12]
10	450	SiO_2	a-Si	[30]
11	430	SiF bending	a-Si:C:F:H	[6]
12	400	SiF bending	a-Si:F:H	[12]

TABLE IV Infrared data in the region ~ 1000–3400 cm^{-1}

Sample no.	Wave number (cm^{-1})	Corresponding assignment	Specimen	Reference
1	3400	Si–OH stretching	a-Si:C:H	[51]
2	3400	Si–OH stretching	a-Si	[37]
3	2900	CH_3 (n = 1, 2, 3) stretching	a-Si:C:H	[51]
4	2900	CH stretching	a-Si:C:F:H	[6]
5	2100	Si-H stretching	a-Si:C:F:H	[6]
6	2000, 2100	SiH_1, SiH_2 stretching	a-Si:H:F	[2]
7	2000, 2100	SiH_1, SiH_2 stretching	a-Si:H:F	[3]
8	2010, 2090	SiH_1–SH_2 stretching	a-Si:H:F	[12]
9	1000–1100	SiO stretching	a-Si	[30]
10	1100–1200	SiO_2 stretching	a-Si	[30]
11	1190	SiO stretching	a-Si:F:H	[2]
12	1200	C–multifluoride stretch	a-Si:C:F:H	[6]
13	1210	$(CH_2)_2SiF_4$	a-Si (electrodeposited)	[4]

bonds has decreased at the higher current density.

There is a shoulder at 1145 cm^{-1} on the left of the peak at 1020 cm^{-1}. Shimizu *et al.* [30] reported the SiO_2 and SiO stretching modes of absorption at 1100–1200 and 1000–1100, respectively. Konagai and Takahashi [2] observed the SiO stretch at 1190 cm^{-1} in a-Si:F:H films. By considering the reports of Paesler *et al.* [32] and others [33–35], on the incorporation of oxygen into hydrogenated a-Si, it may be possible to assign this shoulder absorption to the SiO_2 stretching mode. The shoulder is seen to be broadened in Fig. 3, which may be due to the additional inclusion of the SiO stretching mode [30]. The Si–O–Si structures are absent in these films which, according to Shimizu [30] and Lucovsky and Pollard [36], appear at 940–980 cm^{-1} in a-Si alloys as a very strong, broad absorption. Imura *et al.* [37] reported an absorption at 1070 cm^{-1} due to asymmetric stretching vibrations of Si–O–Si in a-Si films with oxygen incorporation; this is reasonably far from that observed at 1023 cm^{-1}. Obviously, it may also be possible to consider that the 1023 cm^{-1} peak, might have shifted

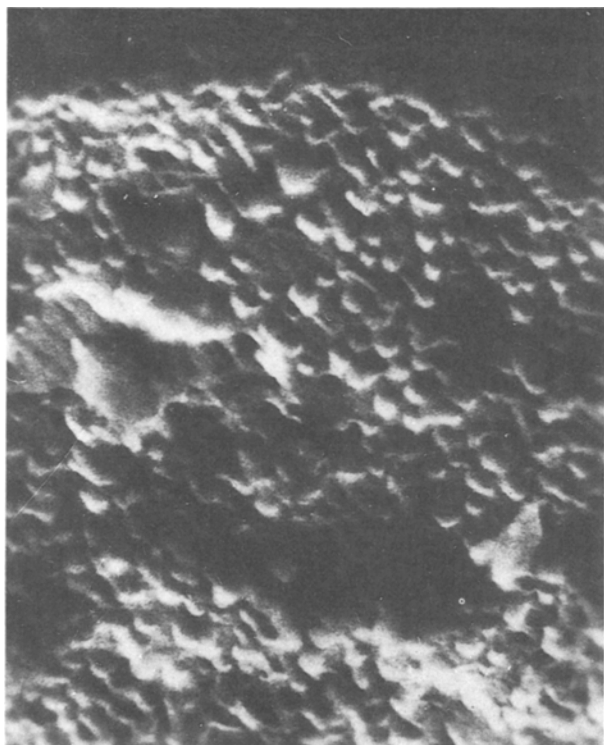

Figure 4 Scanning electron micrograph of Sample 3 with tilted top surface (× 4000).

from the 940–980 cm^{-1} region and hence is attributable to the Si–O–Si stretch mode. The presence of SiF_4 shifts in XPS spectra of these samples (see later) removes this confusion and thus rules out the possibility of an Si–O–Si bridge in the films.

At 1266 cm^{-1}, there is a small spike-like peak. Dyer [38] reported CF stretching at 1000–1400 cm^{-1}. Mohan and Kroger [4] assigned the absorption peak at 1210 cm^{-1} in electrodeposited a-Si to $(CH_2)_2SiF_4$. Morimoto *et al.* [6] observed the C–F (multifluoride) stretch at ~ 1200 cm^{-1}. By considering the studies of Nakazawa *et al.* [39] and Morimoto *et al.* [40] on a-Si:C alloys, it may be possible to assign the observed 1266 cm^{-1} absorption to the CF stretch type.

The weak kink at 920 cm^{-1} in Fig. 1 is due to the Si–H bending mode [1–4, 41]. Small absorption peaks also occur at 730 and 711 cm^{-1}. Meal and Wilson [42] reported the SiC symmetric stretch to be at 553–764 cm^{-1}, whereas Simanouti [43] reported it to be at 695–790 cm^{-1}. Weider *et al.* [44] observed the SiC stretching vibrations at ~ 700 cm^{-1} in a-Si:C films. Also, by following the studies of Borders *et al.* [45] in a-Si:C films and based on the inference that can be drawn for the presence of carbon in a-Si alloys from the chemical bonding model given by Paul *et al.* [46] as discussed below, it may be possible to assign the above peaks at 730 and 711 cm^{-1} to SiC asymmetric and symmetric stretching modes, respectively. It has been emphasized [1] that in a-Si:C:H systems (hydrogen concentrations of 20–30 at %), there is a preferential attachment of hydrogen atoms to the carbon sites. According to Lucovsky [15] and Paul *et al.* [46], this phenomenon may be attributed to the higher bonding energy of C–H compared to Si–H. In this context, it should be noticed that in the above spectra, there are predominant CH stretching modes of absorption at ~ 2900 cm^{-1} compared to that of SiH at ~ 2300 cm^{-1}, as discussed later.

Various other kinks that are seen in Figs 2 and 3 in the region 700–800 cm^{-1} will correspond to CH_x ($x = 1$–3) rocking modes of absorption [14, 44]. There is a small peak at 780 cm^{-1}. Lucovsky [37, 47] and Lucovsky *et al.* [33] reported an absorption at 780 cm^{-1} in a-Si:H:O alloys due to CIS conformation which couples the Si–O–Si and Si–H motions that have a predominantly bond-bending character. However, the absence of Si–O–Si stretching at 940–980 cm^{-1}, as discussed above, emphasizes that the CIS conformation will not hold in the present context. It may be possible to assign the 780 cm^{-1} absorption to CH_3 rocking as in the comparisons of Mohan and Kroger [4], who gave a similar assignment for an observed absorption peak at 770 cm^{-1} in their electrodeposition studies of a-Si. The origin of CH_3 species is the ethylene glycol which, due to dehydration and tautomerization, may become changed to acetaldehyde, and later forms bonds with silane species.

There is a special character in Fig. 2 at 711–828 cm^{-1} containing SiC and SiF stretching modes with a frequency splitting that arises due to the mass difference of carbon and fluorine with respect to the silicon atom. A similar feature is also seen in Fig. 3 at 1025–1150 cm^{-1} where the SiO and SiF stretching modes are usually present. Lucovsky also reported a type of frequency splitting between asymmetric and symmetric stretching modes of SiF_2 and SiF_3 groups in a-Si:H:F alloys due to the increased mass of fluorine relative to hydrogen with respect to silicon, as given by [1, 15]

$$\left(\frac{V_a}{V_s}\right)^2 = \frac{(1 + 2M\sin^2\theta)}{(1 + 2M\cos^2\theta)}\frac{(1 - K)}{(1 + K)} \quad (1)$$

where, V is the frequency, a denotes the symmetric stretching mode, s is the symmetric stretching mode, M is the mass ratio of fluorine to silicon atoms, K is the ratio of the three-body to two-body bond stretching frequencies and 2θ is the Si–F–Si or Si–H–Si bond angle assumed to be equal to the tetrahedral bond angle of 109.47°. For the values and notations given in Reference 1, the fractional splitting has been reported to be 6 cm^{-1}. In a-Si:F also, the splitting of the modes has been observed [15] with a calculated frequency ratio of about 1.10, for the same type of vibrations. In the present study, the line width appears to be 10 cm^{-1} and this phenomenon may be attributable to the fluctuations in the spatial charge distribution due to the complexity of local bonding environments in the vicinity of SiF sites differing with respect to the nature of the atoms or groups that are back bonded to the silicon atom.

In the above figures, small absorption peaks are seen at 635, 677 and 660 cm^{-1}. The 635 cm^{-1} weak absorption is due to the SiH wagging mode according to various authors [2, 12, 15, 18, 48] as given in Table III. Lucovsky *et al.* [33, 47] reported that alloys of the form SiO_2:H with oxygen concentrations substantially larger than the hydrogen concentration, exhibit new vibrations which are derived from sites in which

the hydrogen atom is bonded to the silicon atom that has more than one oxygen atom attached, as in the SiH centre in a-SiO_2. Although the *trans* conformation of oxygen in a-Si:H:O alloys yields absorption modes at 650 and 630 cm^{-1}, involving the bending motions of oxygen and in-plane bending mode of SiH [36, 47], this possibility is ruled out as a choice here, due to the absence of Si–O–Si stretching, as explained above. Ion implantation of oxygen in a-Si displays infrared-active vibrations corresponding to the bending motion of implanted oxygen [49] at 660 cm^{-1}. In addition, on studying post-deposition oxidation in a-Si:H films [35], it may be possible to fix the 677 and 660 cm^{-1} absorptions to H_2SiO_3 and $HSiO_3$, respectively (see reaction mechanisms in Section 4).

According to Mohan and Kroger [4] and the studies of Weider *et al.* [44] and others [39, 40] in a-Si alloys, the 580 and 546 cm^{-1} absorptions are possibly due to CH_xSi_y and to the oxygen in $CH_xSi_yO_z$, respectively. The peak at 505 cm^{-1} may possibly be assigned to the SiTO mode [12]. The region from 500–400 cm^{-1} in the above spectra contains many small peaks of very weak intensity. Amorphous silicon displays a continuum of vibrational modes [1] extending from very low frequencies to about 500 cm^{-1} with no gap region. This implies that virtually all alloy atoms will have one or more vibrations that are resonance modes. Although, it is difficult to trace clearly the absorption peaks below 500 cm^{-1} in the above spectra because of the scale factor, based on the studies of Lucovsky and Tsu [50] and Shimizu *et al.* [30], it may be possible to assign the peak at 485 cm^{-1} to out-of-plane rocking motion of oxygen in a-Si:H:O and that at 450 cm^{-1} to the bending mode of SiO_2. The 470 and 430 cm^{-1} absorptions are due to a-Si and SiF bending, respectively [6, 11].

The strong, broad absorption peak at 3400 cm^{-1} is due to Si–OH stretching as reported by Dyer [38]. Iida and Ohki [51] and Imura *et al.* [37]. The absorptions at 2962, 2927 and 2870 cm^{-1} are due to CH_3, CH_2 and CH_1 stretching modes, respectively [38, 51]. Morimoto *et al.* [6] also observed the CH stretching at 2900 cm^{-1} in a-Si:C:F:H films. In the above figures, a weak absorption is also seen at 2340 cm^{-1}: in a-Si:H alloys, the SiH stretching appears around 2000-2140 cm^{-1} [15, 18]. In a-Si:F:H alloys, Fang *et al.* [12] observed the absorption of SiH and SiH_2 stretching modes at 2020 and 2090 cm^{-1}, respectively; Morimoto *et al.* observed SiH stretching at 2100 cm^{-1} in a-Si:C:F:H films [6]. Lucovsky [52] reported that in substituted silane molecules, the stretching frequency of the SiH group varies from 2315 cm^{-1} in $SiHF_3$ to 2120 cm^{-1} in $SiH(CH_3)_3$. Also, in amorphous solids, it has been shown [15, 52–54] that the SiH bond stretching frequencies vary linearly with the sum of the electronegativities of the atoms or groups that are back bonded to the SiH group. From the infrared studies of SiF_4 by Jones [31] and of substituted silanes by Cradock *et al.* [55] and Newman *et al.* [56, 57], it is possible to assign the ~ 2340 cm^{-1} absorption to SiH stretching in $SiHF_3$, assuming that a few wave numbers shift in electrodeposited systems. In fact, Newman *et al.* [56] observed an absorption peak at 2315 cm^{-1} with medium intensity in the infrared spectra of $SiHF_3$ due to $V_1(a_1)$ local mode vibration, where, V_1 is the fundamental frequency and (a_1) is totally symmetric.

Depending on the symmetry conditions, the $SiHF_3$ molecules exhibit six fundamental frequencies, three totally symmetric (a), and three doubly degenerate (e). The supporting reaction for this assignment is given in Section IV. The absorption peak at 2340 cm^{-1} is stretched lengthwise for about a few wave numbers in Fig. 3. This may be due to the formation of $HSiO_3$ and H_2SiO_3 in the films. The small peak at 1740 cm^{-1} is the resonance mode of $SiHF_3$ [56].

The strong absorption bands at 1600–1620 cm^{-1} in the above figures are due to C–C stretching mode [38, 58, 59]. This reveals strongly the solvent–solute interaction resulting in possible formations such as silane-substituted vinyl ethers. These peaks are extended up to 1730 cm^{-1} on the left side, and may be due to the possible inclusions of C–O stretching modes of absorption [38, 51]. There are various small kinks and peaks in the region from 1500–1300 cm^{-1}, corresponding to bending modes of CH_1, CH_2 and CH_3 groups [1, 38, 44, 51].

Similar absorptions are seen in the spectra of Samples 7, 9, 10 and 13 (Figs 5–8) with a few wave numbers shift in some instances. The above analysis also holds for the spectra of other samples (1, 5, 6, 8, 11 and 12, not shown in the text), but the absorption peaks in the films deposited at low current density are extremely weak. From the observed data, it is evident that more SiF bonds are traced in samples prepared at low concentrations. However, an optimum concentration and current density have been observed in the electrolyte, below which both the deposition rate [8] and the absorption peaks are negligibly small (Samples 1, 5, 6). As the molarity increased from 0.05 M to 0.2 M, although the deposition rate has increased [7, 8], comparatively fewer SiH and SiF bonds are seen in the above spectra, indicating that most of the hydrogen and fluorine gas is lost at the respective electrodes, without becoming bonded to the silicon.

Spike-like features are seen in Fig. 8 at 711 cm^{-1}. As mentioned above, this is under the SiC bond stretching region. This peak is very strong, implying a fundamental mode of absorption with some special character. Borders *et al.* [45] in their ion-implantation studies of carbon in a-Si observed a single absorption band centred at 700 cm^{-1} due to the triplydegenerate bond stretching vibration of the carbon atom. Another phenomenon which should be noted in the present context is that the intensities of CH_x, SiH, SiF_x and C–C modes of absorption in this spectrum are much lower in comparison to that at 711 cm^{-1}. It seems that under the deposition conditions for Sample 13, there is an increased number of carbon atoms that are attached to silicon in the films. This implies further, that under these deposition conditions there are more a-SiC species with carbon atoms sitting in the a-Si host network with a tetrahedral symmetry (Td) [1, 45]. The presence of a medium intensity breathing mode with A_1 symmetry in this spectrum at ~ 495 cm^{-1} supports the above assignment [1].

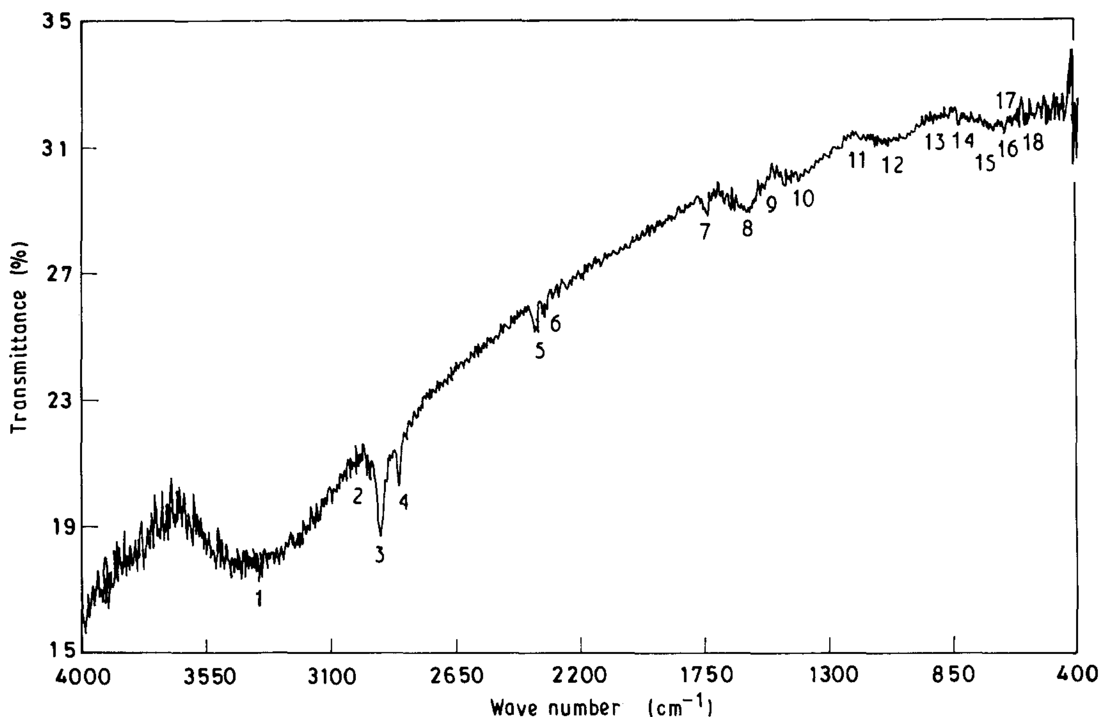

Figure 5 Infrared transmission spectrum of Sample 7. Peak positions (cm^{-1}): (1) 3400, (2) 2962, (3) 2927, (4) 2875, (5) 2335, (6) 2320, (7) 1740, (8) 1612, (9) 1547, 1530, (10) 1456, (11) 1266, (12) 1025, (13) 880, 840, 823, (14) 806, 770, 711, (15) 677, 660, (16) 635, (17) 580, (18) 546, 504, 485, 465, 450, 430.

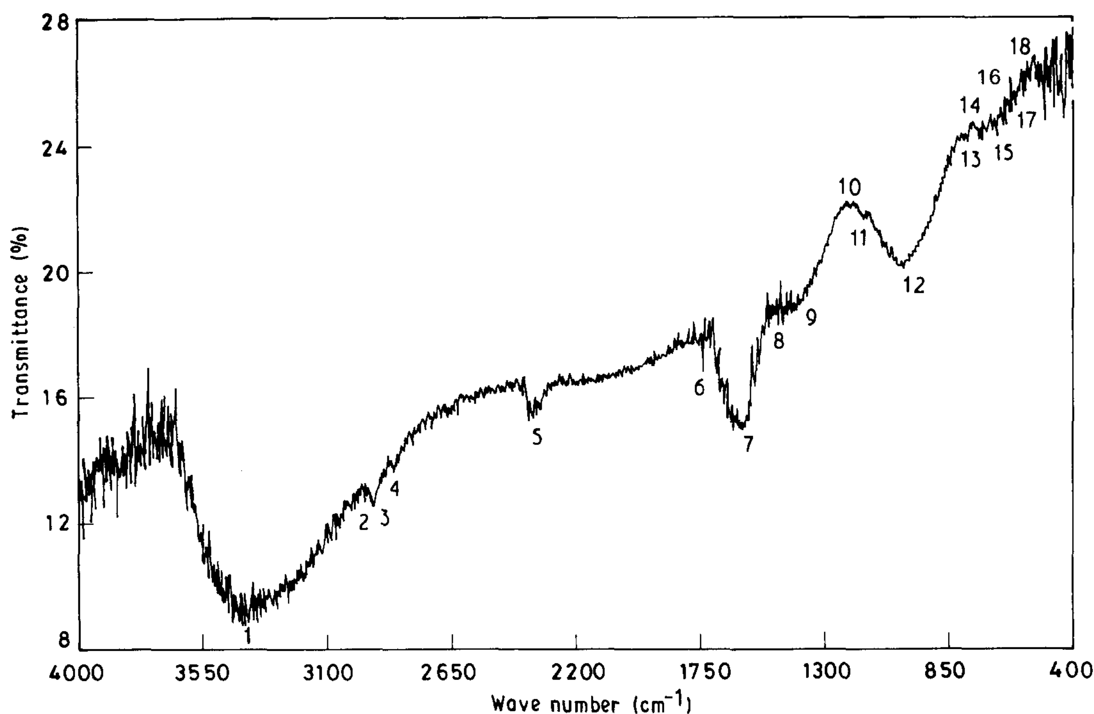

Figure 6 Infrared transmission spectrum of Sample 9. Peak positions (cm^{-1}): (1) 3400, (2) 2962, (3) 2927, (4) 2875, (5) 2336, (6) 1740, (7) 1612, (8) 1470, (9) 1386, (10) 1232, (11) 1150, (12) 1023, (13) 845, 826, 806, (14) 730, 711, (15) 677, 660, (16) 635, (17) 580, 546, (18) 504, 485, 365, 450, 320.

However, the high percentage of carbon atoms may lead to a larger defect density in the films, because of (a) the covalent bond radius of the carbon atom (0.0772 nm) is smaller than that of the silicon atom (0.117 nm), and (b) the flexibility of bond angle for a four-fold coordinated carbon atom is smaller than that for four-fold coordinated silicon atom.

XPS provides information on the core levels of silicon via binding energy shifts. Fig. 9 shows a typical Si–2P spectrum of Sample 13. This spectrum is occupied with unresolved peaks at 99.24, 100.12, 100.8, 102.16, 102.71, 104.6 and 105.7 eV corresponding to SiH, SiC, SiF_1, SiF_2, SiO_2, SiF_3 and SiF_4, respectively [60–62]. These shifts show satisfactory agreement with calculated values obtained from Pauling's ionicity principle [63] and Katayama's value for the proportionality factor ($B = 2.7$) as cited by Katayama [60]. Similar shifts are observed in the XPS spectra of other samples (not shown). Details of the XPS and morphological studies will be published later.

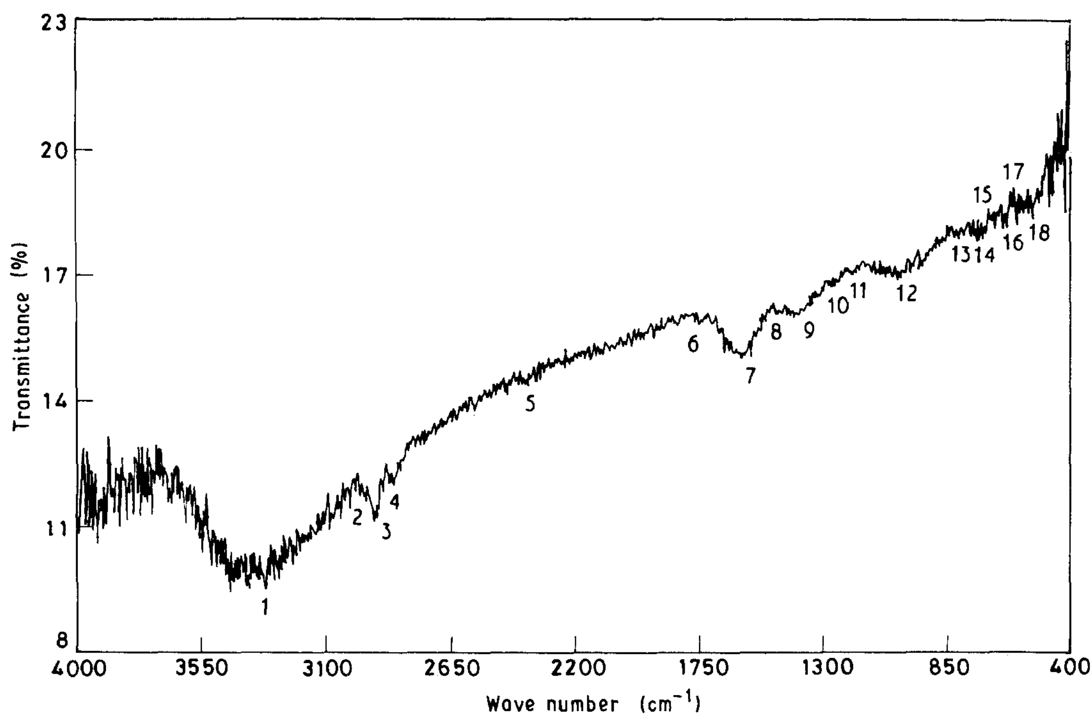

Figure 7 Infrared transmission spectrum of Sample 10. Peak positions (cm^{-1}): (1) 3400, (2) 2962, (3) 2927, (4) 2875, (5) 2338, (6) 1740, (7) 1612, (8) 1456, (9) 1401, (10) 1266, (11) 1127, (12) 1023, (13) 840, 826, 806, (14) 730, 711, (15) 677, 660, (16) 635, (17) 580, 546, (18) 504, 485, 465, 450, 430.

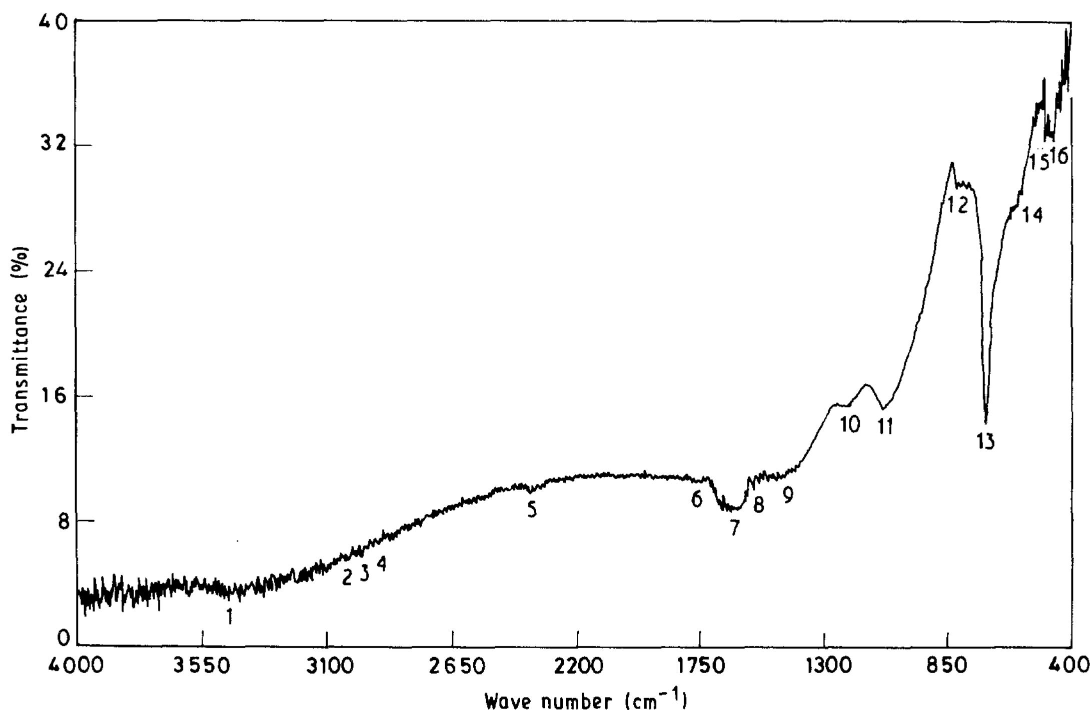

Figure 8 Infrared transmission spectrum of Sample 13. Peak positions (cm^{-1}): (1) 3400, (2) 2962, (3) 2927, (4) 2875, (5) 2335, (6) 1740, (7) 1612, (8) 1540, (9) 1438, (10) 1220, (11) 1029, (12) 833, 826, 806, 746, (13) 711, (14) 635, (15) 504, 495, 465, 430.

The absorption coefficient, α, is shown in Figs 10 and 11 for Samples 3, 4, 9 and 10. From the figures, it is seen that the absorption coefficient in the SiF_2 stretching region has decreased from 2595 cm^{-1} (Fig. 10) to 1380 cm^{-1} (Fig. 11) as the current density increased for the same molarity (0.05 M). Also it is seen that α decreased from 2321 cm^{-1} (Fig. 10) to 1630 cm^{-1} (Fig. 11) as the concentration is increased from 0.1 M to 0.2 M, at the same wave number region as above. The number of hydrogen bonds, N_H, in a sample can be obtained from [40]

$$N_H = A\int \frac{\alpha(W)}{W} dW \qquad (2)$$

where α is the absorption coefficient and W is the wave number. For C–H and Si–H modes in the spectrum

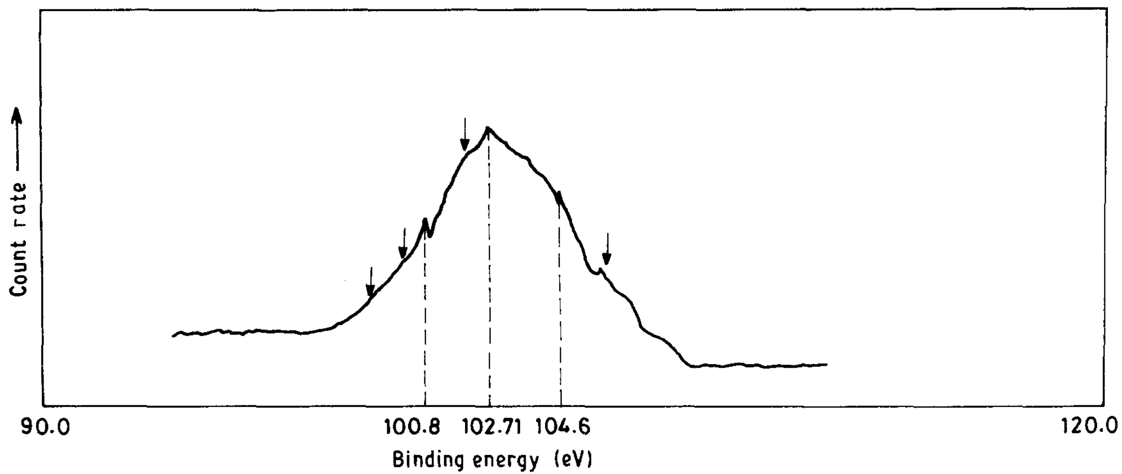

Figure 9 X-ray photoelectron spectra of Sample 13. Source AlK_{α}, ▼ 12.5 kV, 20 mA, 50 eV, 3 mm slits, 300 s, 3×10^3 counts s^{-1}.

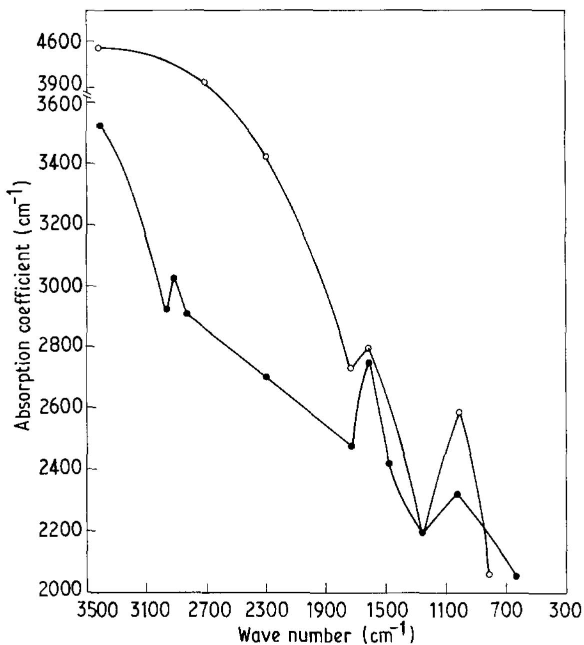

Figure 10 Absorption coefficient of Samples (○) 3 and (●) 9.

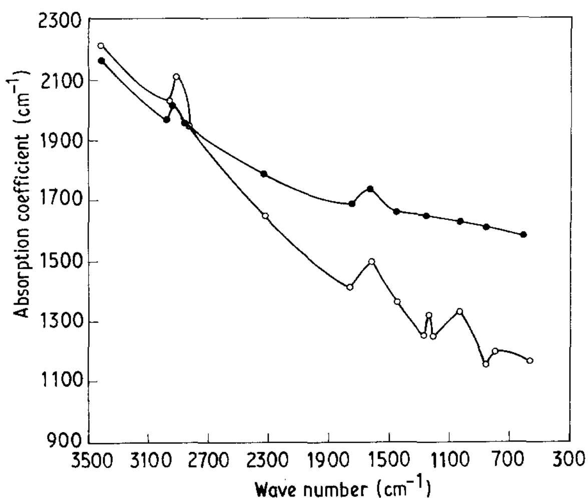

Figure 11 Absorption coefficient of Samples (○) 4 and (●) 10.

of Sample 4, this value has been calculated to be 6.2579×10^{21} and 1.2302×10^{20} atm cm^{-3}, respectively. Here, the value of A is taken approximately as 1.4×10^{20} and 1.7×10^{21} cm^{-2} for Si–H and C–H stretching modes, respectively [40, 64].

4. Possible reactions

The reaction mechanism, for the system using H_2SiF_6, has been reported elsewhere [8]. Some additional reactions that have aided the analysis, are given below.

$$H_2SiF_6 \rightleftharpoons H^+ + HSiF_6^- \quad (3)$$

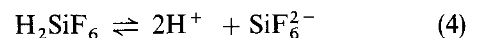

$$H_2SiF_6 \rightleftharpoons 2H^+ + SiF_6^{2-} \quad (4)$$

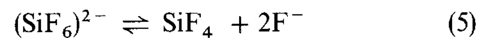

$$(SiF_6)^{2-} \rightleftharpoons SiF_4 + 2F^- \quad (5)$$

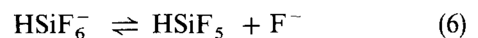

$$HSiF_6^- \rightleftharpoons HSiF_5 + F^- \quad (6)$$

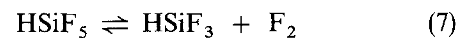

$$HSiF_5 \rightleftharpoons HSiF_3 + F_2 \quad (7)$$

The water present in the solution (H_2SiF_6 is a 60% acid) also ionizes as

$$H_2O \rightleftharpoons H^+ + OH^- \quad (8)$$

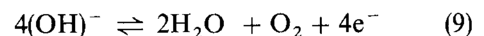

$$4(OH)^- \rightleftharpoons 2H_2O + O_2 + 4e^- \quad (9)$$

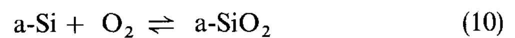

$$\text{a-Si} + O_2 \rightleftharpoons \text{a-SiO}_2 \quad (10)$$

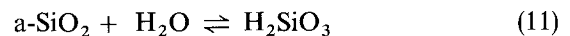

$$\text{a-SiO}_2 + H_2O \rightleftharpoons H_2SiO_3 \quad (11)$$

5. Conclusions

The above observations indicate that films prepared at low molarities contain more fluorine atoms which can serve as dangling bond terminates. There is, of course, an optimum concentration below which the deposition rate is almost negligible. The absence of frequency doublets in infrared spectra, and the absence of columnar growth in the scanning electron micrographs, indicates no polysilane structures in the films. At high concentration and high current densities, the increase in the numbers Si–C bonds (Sample 13) may cause the promotion of larger defect densities in the films. Hence, with proper control of impurities, good quality device-grade a-Si films may be produced by electrodeposition.

Acknowledgements

One of the authors (P.R.L.S.) thanks M. Mosesbabu and R. Padma Kumar for discussions. We thank M. Srinivasa Rao, for assistance while carrying out the experiments, and Professor M. N. Chetty, Department of Metallurgical Engineering, and Professor

G. Basava Raju, Department of Physics, Indian Institute of Technology, Bombay, for their suggestions.

References

1. J. D. JONNOPOULOUS and G. LUCOVSKY (eds) "Topics in Applied Physics; the Physics of Hydrogenated amorphous Silicon". Parts I and II (Springer-Verlag, New York, 1984).
2. M. KONAGAI and TAKAHASHI, *Appl. Phys. Lett.* **36** (1980) 599.
3. S. R. OVSHINSKY and A. MADAN, *Nature* **276** (1978) 482.
4. T. R. RAMA MOHAN and F. A. KROGER, *Electrochem. Acta* **27** (1982) 371.
5. A. SAWADA, S. USUI and M. MIKUCHI, *Jpn J. Appl. Phys.* **20** (1981) PL133.
6. A. MORIMOTO, T. MIURA, M. KUMEDA and T. SHIMIZU, *Jpn Appl. Phys. Part I* **22** (1983) 908.
7. P. R. L. SARMA, I. S. R. SASTRI, V. SINGAL, S. VENKATACHALAM and T. R. RAMA MOHAN, in "Principles of solidification and materials processing", edited by R. Trivedi, J. A. Sekhar and J. Majumdar. Vol. 2 (Oxford and IBH, New Delhi, 1989) pp. 811–818.
8. P. R. L. SARMA, S. VENKATACHALAM and T. R. RAMA MOHAN, *J. Electrochem. Soc. India* **36** (1987) 233.
9. C. H. TINDAL, J. W. STRALEY and H. H. NILESON, *Phys. Rev.* **62** (1942) 151.
10. K. VENKATESWARLU and S. SUNDARAN, *J. Chem. Phys.* **23** (1955) 2365.
11. T. SHIMADA, Y. KATAYAMA and S. HIRIGOME, *Jpn Appl. Phys.* **19** (1980) PL265.
12. C. J. FANG, L. LEY, H. R. SHANKS, K. J. GRUNTZ and G. CARDONA, *Phys. Rev.* **B22** (1980) 6140.
13. G. H. AZARBAYEJANI, R. TSU and G. LUCOVSKY, *Bull. Amer. Phys. Soc.* **28** (1983) 533.
14. H. MATSUMARA, Y. NAKAGOME and S. FURUKAWA, *Appl. Phys. Lett.* **36** (1980) 439.
15. G. LUCOVSKY, "Springer Series in Solid State Science", Vol. 22 (Springer-Verlag, New York, 1981) p. 87.
16. *Idem*, *J. Phys. (Paris) C4* **42** (1981) 741.
17. G. LUCOVSKY, R. J. NEMANICH and J. C. KNIGHTS, *Phys. Rev.* **B19** (1979) 2064.
18. W. B. POLLARD and G. LUCOVSKY, *J. Phys. (Paris) C4* **42** (1981) 353.
19. W. B. POLLARD and J. D. JOANNOPOULOS, *Phys. Rev.* **B23** (1981) 5263.
20. M. A. MADAN, S. R. OVISHINSKY and E. BENN, *Phil. Mag.* **B40** (1979) 259.
21. M. H. BRODSKY, M. CARDONA and J. J. CUOMO, *Phys. Rev.* **B16** (1977) 3556.
22. J. C. KNIGHTS, G. LUCOVSKY and R. J. NEMANICH, *Phil. Mag.* **B37** (1978) 467.
23. W. B. POLLARD and G. LUCOVSKY, *Phys. Rev.* **B26** (1982) 3172.
24. P. JOHN. I. M. ODEH, M. J. K. TOHAMAS and J. I. B. WILSON, *J. Phys. (Paris) C4* **42** (1981) 651.
25. P. JOHN, I. M. ODEH, M. J. K. THOMAS, M. J. TRICKER, F. RIDDOC and J. I. B. WILSON, *Phil. Mag.* **B42** (1980) 671.
26. J. C. KNIGHTS and R. A. LUJAN, *Appl. Phys. Lett.* **35**, (1979) 244.
27. J. C. KNIGHTS, *J. Non-Cryst. Solids* **35/36** (1980) 159.
28. R. J. NEMANICH, D. K. BIEGELSEN and M. P. ROSENBLUM, *J. Phys. Soc. Jpn Suppl.* **A49** (1980) 1189.
29. H. MATSUMARA, K. SAKAI, Y. KAWAKYU and S. FURUKAWA, *J. Appl. Phys.* **52** (1981) 5537.
30. T. SHIMIZU, M. KUMEDA, I. WATANABE and Y. KIRIYAMA, *Jpn. J. Appl. Phys.* **19** (1980) PL235.
31. E. A. JONES, *J. Chem. Phys.* **17** (1951) 242.
32. M. A. PAESLER, D. A. ANDERSON, E. C. FREEMAN, G. MODDEL and W. PAUL, *Phys. Rev. Lett.* **41** (1978) 1492.
33. G. LUCOVSKY, S. S. CHAO, J. FANG, J. E. TYLER and W. CZUBATY, *Phys. Rev.* **B28** (1983) 3225.
34. J. C. KNIGHTS, R. A. STREET and G. LUCOVSKY, *J. Non-Cryst. Solids* **35/36** (1980) 279.
35. P. JOHN. I. M. ODEH, M. J. THOMAS, M. J. TRICKER and J. I. B. WILSON, *Phys. Status Solidi (b)* **105** (1981) 499.
36. G. LUCOVSKY and W. B. POLLARD, *J. Vac. Sci. Technol.* **A1** (1983) 313.
37. T. IMURA, K. USHITA and A. HIRAKI, *Jpn J. Appl. Phys.* **19** (1980) PL650.
38. R. J. DYER, "Applications of absorption spectroscopy of organic compounds" (Prentice Hall, New Delhi, 1974).
39. K. NAKAZAWA, K. SUEDA, M. KUMEDA, A. MORIMOTO and T. SHIMIZU, *Jpn. J. Appl. Phys. Lett.* **21** (1982) PL176.
40. A. MORIMOTO, T. MIURA, M. KUMEDA and T. SHIMIZU, *ibid.* **21** (1982) PL119.
41. J. MAIYASATO, Y. ABE, M. TOKUMURA, T. IMURA and A. HIRAKI, *Jpn J. Appl. Phys.* **22** (1983) PL580.
42. J. H. MEAL and M. K. WILSON, *J. Chem. Phys.* **24** (1956) 385.
43. T. SIMANOUTI, *ibid.* **17** (1949) 245.
44. H. WEIDER, M. CARDONA and C. R. GUARNIERE, *Phys. Status Solidi (b)* **92** (1979) 99.
45. J. A. BORDERS, S. T. PICRANX and W. BEEZHOLD, *Appl. Phys. Lett.* **18** (1971) 509.
46. D. K. PAUL, B. VON ROEDERN, S. OQUZ, J. BLAKE and W. PAUL, *J. Phys. Soc. Jpn Suppl.* **A49** (1980) 1261.
47. G. LUCOVSKY, *Sol. Energy Mater.* **8** (1982) 165.
48. E. C. FREEMAN and W. PAUL, *Phys. Rev. B18* (1978) 4288.
49. G. LUCOVSKY and R. TSU, in "Topics in Applied Physics: the Physics of Hydrogenated Amorphous Silicon", Part II, edited by J. D. Jonnopoulous and G. Lucovsky (Springer-Verlag, New York, 1984) p. 342.
50. G. LUCOVSKY and R. TSU, *ibid.*, Part II, p. 346.
51. S. IIDA and S. OHKI, *Jpn J. Appl. Phys.* **21** (1982) PL62.
52. G. LUCOVSKY, *Solid State Commun.* **29**, (1979) 571.
53. A. L. SMITH and N. C. ANGELOTTI, *Spectrochem. Acta* **15** (1959) 412.
54. H. W. THOMPSON, *ibid.* **16** (1959) 412.
55. S. CRADOCK, E. A. V. EBSWORTH and A. G. ROBBIETTE, *Trans. Faraday Soc.* **60** (1964) 502.
56. C. NEWMAN, S. R. POLO and M. K. WILSON, *Spectrochem. Acta* **59** (1959) 793.
57. C. NEWMAN, J. K. BLOANE, S. R. POLO and M. K. WILSON, *J. Chem. Phys.* **25** (1956) 855.
58. A. P. ALTSHULLER, *ibid.* **23** (1955) 761.
59. R. N. KNISELEY, V. A. FASSET and E. E. CONARD, *ibid.* **27** (1959) 651.
60. Y. KATAYAMA, K. USAMI and T. SHIMADA, *Phil. Mag.* **B43** (1981) 283.
61. L. LEY, K. J. GRUNTZ, R. L. JOHNSON, in "Tetrahedrally Bonded Amorphous Semiconductors", edited by R. A. Street, D. K. Biegelsen, J. C. Knights (American Institute of Physics, New York, 1981) p. 161.
62. N. FUKADA, *Jpn J. Appl. Phys. Part II* **22** (1983) 745.
63. L. PAULING, "The Nature of Chemical Bonds" (Cornell University Press, New York, 1960) p. 85.
64. C. J. FANG, *J. Non-Cryst. Solids* **35/36** (1980) 225.

Received 1 May
and accepted 12 September 1991